
Distilling importance sampling

Dennis Prangle¹

Abstract

The two main approaches to Bayesian inference are sampling and optimisation methods. However many complicated posteriors are difficult to approximate by either. Therefore we propose a novel approach combining features of both. We use a flexible parameterised family of densities, such as a normalising flow. Given a density from this family approximating the posterior, we use importance sampling to produce a weighted sample from a more accurate posterior approximation. This sample is then used in optimisation to update the parameters of the approximate density, which we view as distilling the importance sampling results. We iterate these steps and gradually improve the quality of the posterior approximation. We illustrate our method in two challenging examples: a queueing model and a stochastic differential equation model.

1. Introduction

Bayesian inference has had great success in recent decades (Green et al., 2015), but remains challenging in models with a complex posterior dependence structure e.g. those involving *latent variables*. Monte Carlo methods are one state-of-the-art approach. These produce samples from the posterior distribution. However in many settings it remains challenging to design good mechanisms to propose plausible samples, despite many advances (Cappé et al., 2004; Cornuet et al., 2012; Graham & Storkey, 2017; Whitaker et al., 2017).

We focus on one simple Monte Carlo method: *importance sampling* (IS). This weights draws from a *proposal distribution* so that the weighted sample can be viewed as representing a *target distribution*, such as the posterior. IS can be used in almost any setting, including in the presence of strong posterior dependence or discrete random variables. However it only achieves a representative weighted sample

at a feasible cost if the proposal is a reasonable approximation to the target distribution.

An alternative to Monte Carlo is to use optimisation to find the best approximation to the posterior from a family of distributions. Typically this is done in the framework of *variational inference* (VI). VI is computationally efficient but has the drawback that it often produces poor approximations to the posterior distribution e.g. through over-concentration (Turner et al., 2008; Yao et al., 2018).

A recent improvement in VI is due to the development of a range of flexible and computationally tractable distributional families using *normalising flows* (Dinh et al., 2016; Papamakarios et al., 2019a). These transform a simple base random distribution to a complex distribution, using a sequence of learnable transformations.

We propose an alternative to variational inference for training the parameters of an approximate posterior density, typically a normalising flow, which we call the *distilled density*. This alternates two steps. The first is importance sampling, using the current distilled density as the proposal. The target distribution is an approximate posterior, based on *tempering*, which is an improvement on the proposal. The second step is to use the resulting weighted sample to train the distilled density further. Following Li et al. (2017), we refer to this as *distilling* the importance sampling results. By iteratively distilling IS results, we can target increasingly accurate posterior approximations i.e. reduce the amount of tempering.

Each step of our *distilled importance sampling* (DIS) method aims to reduce the Kullback Leibler (KL) divergence of the distilled density from the current tempered posterior. This is known as the *inclusive* KL divergence, as minimising it tends to produce a density which is over-dispersed compared to the tempered posterior. Such a distribution is well suited to be an IS proposal distribution.

In the remainder of the paper, Section 2 presents background on Bayesian inference and normalising flows. Sections 3 and 4 describe our method. Section 5 illustrates it on a simple two dimensional inference task. Sections 6 and 7 give more challenging examples: queueing and time series models. Section 8 concludes with a discussion, including limitations and opportunities for future improvements.

¹School of Mathematics, Statistics and Physics, Newcastle University, Newcastle, United Kingdom. Correspondence to: Dennis Prangle <dennis.prangle@newcastle.ac.uk>.

A link to code for the examples will be included in the final version of this paper. All examples were run on a 6-core desktop PC.

Related work Several recent papers (Müller et al., 2018; Cotter et al., 2019; Duan, 2019) learn a density defined via a transformation to use as an importance sampling proposal. A novelty of our work is using a sequential approach based on tempering.

A related approach is to distill Markov chain Monte Carlo output, but this turns out to be more difficult than for IS. One reason is that optimising the KL divergence typically requires unbiased estimates of it or related quantities (e.g. its gradient), but MCMC only provides unbiased estimates asymptotically. Li et al. (2017) and Parno & Marzouk (2018) proceed by using biased estimates, while Ruiz & Titsias (2019) introduce an alternative more tractable divergence. However IS, as we shall see, can produce unbiased estimates of the required KL gradient.

Approximate Bayesian computation (ABC) methods (Marin et al., 2012; Del Moral et al., 2012) involve simulating datasets under various parameters to find those which produce close matches to the observations. However, close matches are rare unless the observations are low dimensional. Hence ABC typically uses dimension reduction of the observations through *summary statistics*, which reduces inference accuracy. Our method can instead learn a joint proposal distribution for the parameters and all the random variables used in simulating a dataset (see Section 6 for details). Hence it can *control* the simulation process to frequently output data similar to the full observations.

Conditional density estimation methods (see e.g. Le et al., 2017, Papamakarios et al., 2019b, Grazian & Fan, 2019) fit a joint distribution to parameters and data from simulations. Then one can condition on the observed data to approximate its posterior distribution. These methods also sometimes require dimension reduction, and can perform poorly when the observed data is unlike the simulations. Our approach avoids these difficulties by directly finding parameters which can reproduce the full observations.

More broadly, DIS has connections to several inference methods. Concentrating on its IS component, it is closely related to *adaptive importance sampling* (Cornuet et al., 2012) and *sequential Monte Carlo* (SMC) (Del Moral et al., 2006). Concentrating on training an approximate density, it can be seen as a version of the *cross-entropy method* (Rubinstein, 1999) or an *estimation of distribution* algorithm (Larrañaga & Lozano, 2002).

2. Background

This section presents background on Bayesian inference and normalising flows.

2.1. Bayesian framework

We observe data y , assumed to be the output of a probability model $p(y|\theta)$ under some parameters θ . Given prior density $\pi(\theta)$ we aim to find corresponding posterior $p(\theta|y)$.

Many probability models involve latent variables x , so that $p(y|\theta) = \int p(y|\theta, x)p(x|\theta)dx$. To avoid computing this integral we'll attempt to infer the joint posterior $p(\theta, x|y)$, and marginalise to get $p(\theta|y)$. For convenience we introduce $\xi = (\theta, x)$ to represent the collection of parameters and latent variables. For models without latent variables $\xi = \theta$.

We now wish to infer $p(\xi|y)$. Typically we can only evaluate an *unnormalised* version,

$$\tilde{p}(\xi|y) = p(y|\theta, x)p(x|\theta)\pi(\theta).$$

Then $p(\xi|y) = \tilde{p}(\xi|y)/Z$ where $Z = \int \tilde{p}(\xi|y)d\xi$ is an intractable *normalising constant*.

2.2. Tempering

We'll use a *tempered* target density $p_\epsilon(\xi)$ such that p_0 is the posterior and $\epsilon > 0$ gives an approximation. As for the posterior, we can often only evaluate an unnormalised version $\tilde{p}_\epsilon(\xi)$. Then $p_\epsilon(\xi) = \tilde{p}_\epsilon(\xi)/Z_\epsilon$ where $Z_\epsilon = \int \tilde{p}_\epsilon(\xi)d\xi$. We use various tempering schemes later in the paper: see (8), (9) and (12).

2.3. Importance sampling

Let $p(\xi)$ be a target density, such as a tempered posterior, where $p(\xi) = \tilde{p}(\xi)/Z$ and only $\tilde{p}(\xi)$ can be evaluated. Importance sampling (IS) is a Monte Carlo method to estimate expectations of the form

$$I = \mathbb{E}_{\xi \sim p}[h(\xi)],$$

for some function h . Here we give an overview of relevant aspects. For full details see e.g. Robert & Casella (2013) and Rubinstein & Kroese (2016).

IS requires a *proposal density* $\lambda(\xi)$ which can easily be sampled from, and must satisfy

$$\text{supp}(p) \subseteq \text{supp}(\lambda), \quad (1)$$

where supp denotes support. Then

$$I = \mathbb{E}_{\xi \sim \lambda} \left[\frac{p(\xi)}{\lambda(\xi)} h(\xi) \right]. \quad (2)$$

So an unbiased Monte Carlo estimate of I is

$$\hat{I}_1 = \frac{1}{NZ} \sum_{i=1}^N w_i h(\xi^{(i)}), \quad (3)$$

where $\xi^{(1)}, \xi^{(2)}, \dots, \xi^{(N)}$ are independent samples from λ , and $w_i = \tilde{p}(\xi^{(i)})/\lambda(\xi^{(i)})$ gives a corresponding *importance weight*.

Typically Z is estimated as $\frac{1}{N} \sum_{i=1}^N w_i$ giving

$$\hat{I}_2 = \frac{\sum_{i=1}^N w_i h(\xi^{(i)})}{\sum_{i=1}^N w_i}, \quad (4)$$

a biased, but consistent, estimate of I . Equivalently

$$\hat{I}_2 = \frac{\sum_{i=1}^N s_i h(\xi^{(i)})}{\sum_{i=1}^N s_i},$$

for *normalised* importance weights $s_i = w_i / \sum_{i=1}^N w_i$.

A drawback of importance sampling is that it can produce estimates with large, or infinite, variance if λ is a poor approximation to p . Hence diagnostics for the quality of the results are useful.

A popular diagnostic is *effective sample size* (ESS),

$$N_{\text{ESS}} = \frac{\left(\sum_{i=1}^N w_i \right)^2}{\sum_{i=1}^N w_i^2}. \quad (5)$$

For most functions h , $\text{Var}(\hat{I}_2)$ roughly equals the variance of an idealised Monte Carlo estimate based on N_{ESS} independent samples from $p(\xi)$ (Liu, 1996).

2.4. Normalising flows

A *normalising flow* represents a random vector ξ with a complicated distribution as an invertible transformation of a random vector z with a simple *base distribution*, typically $\mathcal{N}(0, I)$. A simple example is an *autoregressive model* where $\xi_i = f(\xi_{i-1}, z_i)$ for some suitable f . See Section 7 for a time series example.

Recent research has developed flexible learnable families of normalising flows. See Papamakarios et al. (2019a) for a review. We focus on real NVP (“non-volume preserving”) flows (Dinh et al., 2016). These compose several transformations of z . One type is a *coupling layer* which transforms input vector u to output vector v , both of dimension D , by

$$\begin{aligned} v_{1:d} &= u_{1:d}, & v_{d+1:D} &= \mu + \exp(\sigma) \odot u_{d+1:D}, \\ \mu &= f_\mu(u_{1:d}), & \sigma &= f_\sigma(u_{1:d}), \end{aligned}$$

where \odot and \exp are elementwise multiplication and exponentiation. Here the first d elements of u are copied unchanged. We typically take $d = \lfloor \frac{1}{2}D \rfloor$. The other elements are scaled by vector $\exp(\sigma)$ then shifted by vector μ , where μ and σ are functions of $u_{1:d}$. This transformation is invertible, and allows quick computation of the density of v from that of u , as the Jacobian determinant is simply

$\prod_{i=d+1}^D \exp(\sigma_i)$. Coupling layers are alternated with permutations so that different variables are copied in successive coupling layers. Real NVP typically uses order-reversing or random permutations.

The functions f_μ and f_σ are neural network outputs. Each coupling layer has its own neural network. The collection of all weights and biases, ϕ , can be trained for particular tasks e.g. density estimation of images. Permutations are fixed in advance and not learnable.

Real NVP produces a flexible family of densities $q(\xi; \phi)$ with two useful properties for this paper. Firstly, samples can be drawn rapidly. Secondly, it is reasonably fast to compute $\nabla_\phi \log q(\xi; \phi)$ for any ξ .

3. Objective and gradient

Given an approximate family of densities $q(\xi; \phi)$, such as normalising flows, this section introduces objective functions to judge how well q approximates a tempered posterior p_ϵ . It then discusses how to estimate the gradient of this objective with respect to ϕ . Section 4 presents our algorithm using these gradients to sequentially update ϕ while also reducing ϵ .

3.1. Objective

Given p_ϵ , we aim to minimise the inclusive Kullback-Leibler (KL) divergence,

$$KL(p_\epsilon || q) = \mathbb{E}_{\xi \sim p_\epsilon} [\log p_\epsilon(\xi) - \log q(\xi; \phi)].$$

This is equivalent to maximising a scaled negative *cross-entropy*, which we use as our objective,

$$\mathcal{J}_\epsilon(\phi) = Z_\epsilon \mathbb{E}_{\xi \sim p_\epsilon} [\log q(\xi; \phi)].$$

(We scale by Z_ϵ to avoid this intractable constant appearing in our gradient estimates below.)

The inclusive KL divergence penalises ϕ values which produce small $q(\xi; \phi)$ when $p_\epsilon(\xi)$ is large. Hence the optimal ϕ tends to make $q(\xi; \phi)$ non-negligible where $p_\epsilon(\xi)$ is non-negligible, known as the *zero-avoiding* property. This is an intuitively attractive feature for importance sampling proposal distributions. Indeed recent theoretical work shows that, under some conditions, the sample size required in importance sampling scales exponentially with the inclusive KL divergence (Chatterjee & Diaconis, 2018).

Our work could be adapted to use the χ^2 divergence (Dieng et al., 2017; Müller et al., 2018), which also has theoretical links to the sample size required by IS (Agapiou et al., 2017).

3.2. Basic gradient estimate

Assuming standard regularity conditions (Mohamed et al., 2019, Section 4.3.1), the objective has gradient

$$\nabla \mathcal{J}_\epsilon(\phi) = Z_\epsilon \mathbb{E}_{\xi \sim p_\epsilon} [\nabla \log q(\xi; \phi)].$$

Using (2), an importance sampling form is

$$\nabla \mathcal{J}_\epsilon(\phi) = \mathbb{E}_{\xi \sim \lambda} \left[\frac{\tilde{p}_\epsilon(\xi)}{\lambda(\xi)} \nabla \log q(\xi; \phi) \right],$$

where $\lambda(\xi)$ is a proposal density. We will take $\lambda(\xi) = q(\xi; \phi^*)$ for some ϕ^* . (In our main algorithm, ϕ^* will be the output of a previous optimisation step.) Note we use choices of q with full support, so (1) is satisfied.

An unbiased Monte Carlo gradient estimate is

$$g_1 = \frac{1}{N} \sum_{i=1}^N w_i \nabla \log q(\xi^{(i)}; \phi), \quad (6)$$

where $\xi^{(i)} \sim \lambda(\xi)$ are independent samples and $w_i = \tilde{p}_\epsilon(\xi^{(i)})/\lambda(\xi^{(i)})$ are importance sampling weights.

We calculate $\nabla \log q(\xi^{(i)}; \phi)$ by backpropagation. Note we backpropagate with respect to ϕ , but not ϕ^* which is treated as a constant. Hence the $\xi^{(i)}$ values are themselves constant.

3.3. Improved gradient estimates

Here we discuss reducing the variance and cost of g_1 .

Clipping weights To avoid high variance gradient estimates we apply *truncated importance sampling* (Ionides, 2008). This clips the weights at a maximum value ω , producing truncated importance weights $\tilde{w}_i = \min(w_i, \omega)$. The resulting gradient estimate is

$$g_2 = \frac{1}{N} \sum_{i=1}^N \tilde{w}_i \nabla \log q(\xi^{(i)}; \phi).$$

This typically has lower variance than g_1 , but has some bias. See Appendix A for more details and discussion, including how we choose ω automatically.

Resampling The gradient estimate g_2 requires calculating $\nabla \log q(\xi^{(i)}; \phi)$ for $1 \leq i \leq N$. Each of these has an associated computational cost, but often many receive small weights and so contribute little to g_2 .

To reduce this cost we can discard many low weight samples, by using *importance resampling* (Smith & Gelfand, 1992) as follows. We sample $n \ll N$ times, with replacement, from the $\xi^{(j)}$ s with probabilities $\tilde{s}_j = \tilde{w}_j/S$ where $S = \sum_{i=1}^N \tilde{w}_i$. Denote the resulting samples as $\tilde{\xi}^{(j)}$. The following is then an unbiased estimate of g_2 ,

$$g_3 = \frac{S}{nN} \sum_{j=1}^n \nabla \log q(\tilde{\xi}^{(j)}; \phi). \quad (7)$$

4. Algorithm

Our approach to inference is as follows. Given a current distilled density approximating the posterior, $q(\xi; \phi_t)$, we use this as $\lambda(\xi)$ in (7) to produce a gradient estimate. (In the notation of Section 3.2, we take $\phi^* = \phi_t$.) We then update ϕ_t to ϕ_{t+1} by stochastic gradient ascent, aiming to increase \mathcal{J}_ϵ . As t increases, we also reduce the tempering in our target density $p_\epsilon(\xi)$ by reducing ϵ , slowly enough to avoid high variance gradient estimates.

Algorithm 1 gives our implementation of this approach. The remainder of the section discusses various details of it. See Appendix G for a discussion of algorithm complexity.

Algorithm 1 Distilled importance sampling (DIS)

- 1: Input: importance sampling size N , target ESS M , batch size n , initial tempering parameter ϵ_0
 - 2: Initialise ϕ_0 (followed by pretraining if necessary).
 - 3: **for** $t = 1, 2, \dots$ **do**
 - 4: Sample $(\xi_i)_{1 \leq i \leq N}$ from $q(\xi; \phi_{t-1})$.
 - 5: Select a new tempering parameter $\epsilon_t \leq \epsilon_{t-1}$ (see Section 4.2 for details).
 - 6: Calculate weights $w_i = \tilde{p}_\epsilon(\xi^{(i)})/q(\xi^{(i)}; \phi_{t-1})$ and truncate to \tilde{w}_i s (see Appendix A for details).
 - 7: **for** $j = 1, 2, \dots, B$ **do**
 - 8: Resample $(\tilde{\xi}^{(j)})_{1 \leq j \leq n}$ from $(\xi^{(i)})_{1 \leq i \leq N}$ using normalised \tilde{w}_i s as probabilities, with replacement.
 - 9: Calculate gradient estimate g_3 using (7).
 - 10: Update ϕ using stochastic gradient optimisation. We use the Adam algorithm.
 - 11: **end for**
 - 12: **end for**
-

We fix training batch size to $n = 100$, and number of batches B to M/n . So steps 4–6 perform importance sampling with a target ESS of M . Then steps 7–11 uses M of its outputs (sampled with replacement) for training. The idea is to avoid overfitting by too much reuse of the same training data.

We investigate other tuning choices for the algorithm in Section 6. For now note that N must be reasonably large since our method to update ϵ_t relies on making an accurate ESS estimate, as detailed in Section 4.2.

4.1. Initialisation and pretraining

The initial q should be similar to the initial target p_{ϵ_0} . Otherwise the first gradient estimates produced by importance sampling are likely to be high variance. We can sometimes be achieved by initialising ϕ to give q a particular distribution, and designing our tempering scheme to have a similar initial target. See Appendix B for details, and Sections 5–7 for examples.

Pretraining can also be used to improve the match between

the initial q and p_{ϵ_0} when it is possible to sample from the latter. This iterates the following steps:

1. Sample $(\xi^{(i)})_{1 \leq i \leq n}$ from $p_{\epsilon_0}(\xi)$.
2. Update ϕ using gradient $\frac{1}{n} \sum_{i=1}^n \nabla \log q(\xi^{(i)}; \phi)$.

This aims to maximise the negative cross-entropy $E_{\xi \sim p_{\epsilon_0}}[\log q(\xi; \phi)]$. We use $n = 100$, and terminate once $q(\xi; \phi)$ achieves a reasonable ESS (e.g. half actual sample size) when targeting p_{ϵ_0} in importance sampling.

4.2. Selecting ϵ_t

We select ϵ_t using effective sample size, as in [Del Moral et al. \(2012\)](#). Given $(\xi_i)_{1 \leq i \leq N}$ sampled from $q(\xi; \phi_{t-1})$, the resulting ESS value for target $p_\epsilon(\xi)$ is

$$N_{\text{ESS}}(\epsilon) = \frac{[\sum_{i=1}^N w(\xi_i, \epsilon)]^2}{\sum_{i=1}^N w(\xi_i, \epsilon)^2}, \text{ where } w(\xi, \epsilon) = \frac{\tilde{p}_\epsilon(\xi)}{q(\xi; \phi_{t-1})}.$$

In step 5 of [Algorithm 1](#) we first check whether $N_{\text{ESS}}(\epsilon_{t-1}) < M$, where M is the target ESS value. If so we take $\epsilon_t = \epsilon_{t-1}$. Otherwise we let ϵ_t be an estimate of the minimal ϵ such that $N_{\text{ESS}}(\epsilon) \geq M$, computed by a bisection algorithm.

5. Example: sinusoidal distribution

As a simple illustration, consider $\theta_1 \sim U(-\pi, \pi)$, $\theta_2 | \theta_1 \sim \mathcal{N}(\sin(\theta_1), 1/200)$, giving unnormalised target density

$$\tilde{p}(\theta) = \exp\{-100[\theta_2 - \sin(\theta_1)]^2\} \mathbb{1}[|\theta_1| < \pi],$$

where $\mathbb{1}$ is an indicator function. (Note earlier sections infer $\xi = (\theta, x)$, where x are latent variables. This example has no latent variables, so we simply infer θ .)

We use the unnormalised tempered target

$$\tilde{p}_\epsilon(\theta) = p_1(\theta)^\epsilon \tilde{p}(\theta)^{1-\epsilon}, \quad (8)$$

initialising ϵ at 1 and reducing it to 0 during the algorithm.

As initial distribution we take θ_1 and θ_2 to have independent $\mathcal{N}(0, \sigma_0^2)$ distributions. We use $\sigma_0 = 2$ to give a reasonable match to the standard deviation of θ_1 under the target. Hence

$$p_1(\theta) = \frac{1}{2\pi\sigma_0^2} \exp\left[-\frac{1}{2\sigma_0^2}(\theta_1^2 + \theta_2^2)\right].$$

We use real NVP for $q(\theta; \phi)$, with 4 coupling layers, alternated with permutation layers swapping θ_1 and θ_2 . Each coupling layer uses a neural network with 3 hidden layers of 10 hidden units each and ELU activation. We initialise q close to a $\mathcal{N}(0, I)$ distribution, as in [Appendix B](#), then pretrain so q approximates p_1 .

We use [Algorithm 1](#) with $N = 4000$ training samples and a target ESS of $M = 2000$. These values are chosen to produce a clear visual illustration: we investigate efficient tuning choices later.

[Figure 1](#) shows our results. The distilled density quickly adapts to meet the importance sampling results, and $\epsilon = 0$ is reached by 90 iterations. This took roughly 1.5 minutes.

6. Example: M/G/1 queue

This section describes an application to *likelihood-free inference* ([Marin et al., 2012](#); [Papamakarios & Murray, 2016](#)). Here a generative model or *simulator* is specified, typically by computer code. This maps parameters θ and pseudo-random draws x to data $y(\theta, x)$.

Given observations y_0 , we aim to infer the joint posterior of θ and x , $p(\xi|y_0)$. In this section we approximate this with a *black-box* choice of $q(\xi|\phi)$ i.e. a generic normalising flow. This approach could be applied to any simulator model without modifying its computer code, instead overriding the random number generator to use x values proposed by q , as in [Baydin et al. \(2019\)](#). However, for higher dimensional (θ, x) a black-box approach becomes impractical. [Section 7](#) outlines an alternative – using knowledge of the simulator to inform the choice of q .

6.1. Model

We consider a M/G/1 queuing model. This is based on a single queue of customers. Times between arrivals at the back of the queue are $Exp(\theta_1)$. Upon reaching the front of the queue, a customer’s service time is $U(\theta_2, \theta_3)$. All these random variables are independent.

We consider a setting where only *inter-departure times* are observed: times between departures from the queue. This model is a common benchmark for likelihood-free inference, which can often provide fast approximate inference. See [Papamakarios et al. \(2019b\)](#) for a detailed comparison. An advantage of DIS over these methods is that it does not require using low dimensional summary statistics which lose some information from the data. Near-exact posterior inference is also possible for this model using a sophisticated MCMC scheme ([Shestopaloff & Neal, 2014](#)).

We sample a synthetic dataset of $m = 20$ observations from parameter values $\theta_1 = 0.1, \theta_2 = 4, \theta_3 = 5$. We attempt to infer these parameters under the prior $\theta_1 \sim U(0, 1/3), \theta_2 \sim U(0, 10), \theta_3 - \theta_2 \sim U(0, 10)$ (all independent).

6.2. DIS implementation

Latent variables and simulator We introduce ϑ and x , vectors of length 3 and $2m$, and take ξ as the collection (ϑ, x) . Our simulator transforms these inputs to $\theta(\vartheta)$ and

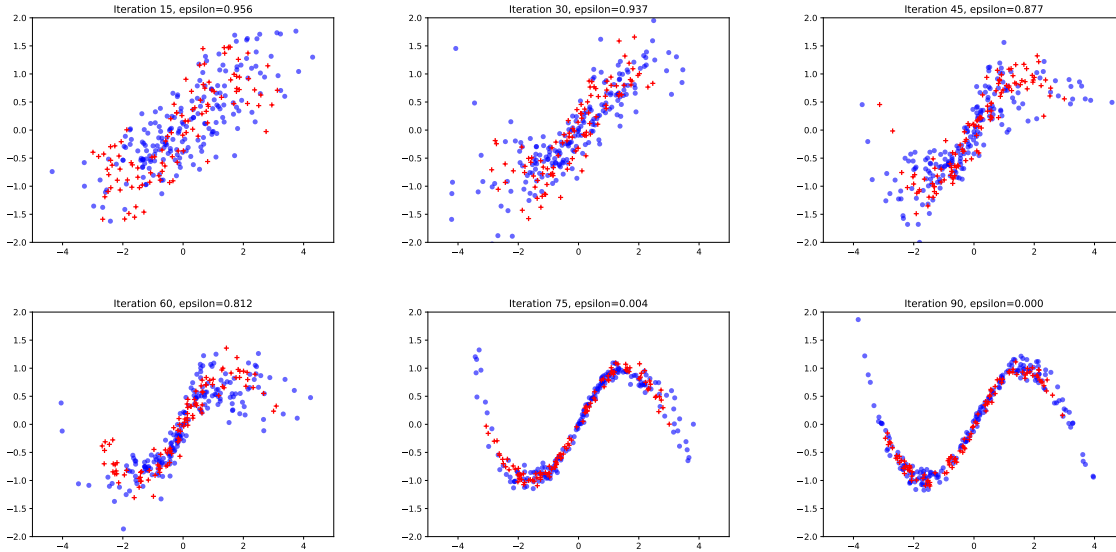


Figure 1. Training output for sinusoidal example. Each frame shows 300 samples from the current distilled density. A subsample of 150 targeting $p_\epsilon(\theta)$ for the current ϵ value is selected by importance resampling (see Section 3.3) and shown as red crosses. The remaining points are shown as blue dots.

$y(\xi)$. We do this in such a way that when the ξ elements have independent $\mathcal{N}(0, 1)$ distributions, then (θ, y) is a sample from the prior and the model. See Appendix C for details.

Tempered target Our unnormalised tempered target is

$$\tilde{p}_\epsilon(\xi) = \pi(\theta) \exp\left[-\frac{1}{2\epsilon^2}d(\xi)^2\right], \quad \text{for } \epsilon > 0 \quad (9)$$

where $d(\xi) = \|y(\xi) - y_0\|_2$ is the Euclidean distance between the simulated and observed data. This target is often used in ABC and corresponds to the posterior under the assumption that the data is observed with independent $\mathcal{N}(0, \epsilon^2)$ errors (Wilkinson, 2013). We use initial value $\epsilon_0 = 10$: a scale for errors which is large relative to our observations. Note that DIS cannot reach the exact target here. Instead, like ABC, it will produce increasingly good posterior approximations as $\epsilon \rightarrow 0$.

Tuning choices We use a real NVP architecture for $q(\xi; \phi)$ with 16 coupling layers alternated with random permutation layers. Each coupling layer uses a neural network with 3 hidden layers of 100, 100, 50 units and ELU activation. We initialise q close to a $\mathcal{N}(0, I)$ distribution, as described in Appendix B. This is close enough to the initial target that pretraining was not needed.

6.3. Results

Figure 2 compares different choices of N (number of importance samples) and M (target ESS). It shows that ϵ reduces

more quickly for larger N or smaller M . Our choice of N was restricted by memory requirements: the largest value we used was 50,000. Our choice of M was restricted by numerical stability: values below a few hundred often produced numerical overflow errors in the normalising flow.

This tuning study suggests using large N and small M subject to these restrictions. We use this guidance here and in Section 7. In both examples, the cost of a single evaluation of the target density is low. For more expensive models efficient tuning choices may differ.

Figure 3 shows that DIS results with $N = 50,000$ and $M = 2500$ are a close match to near-exact MCMC output using the algorithm of Shestopaloff & Neal (2014). The main difference is that DIS lacks sharp truncation at $\theta_2 = 4$.

7. Example: Lorenz model

Here we consider a time series application. Noisy and infrequent observations y of a time series path x are available. The black-box approach of Section 6 is not practical here: $\dim(x)$ is too large to learn (θ, x) directly. Instead we take an amortised approach, exploiting knowledge of the model structure by just learning $q(\theta)$ (marginal parameters) and $q(x_{i+1}|x_i, \theta)$ (next step of the time series).

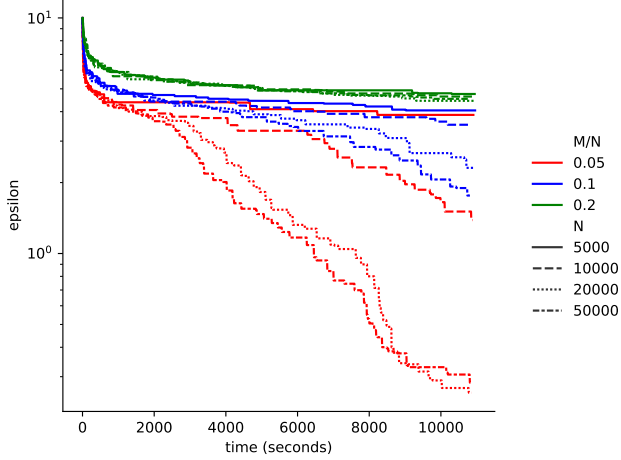


Figure 2. The ϵ value reached by DIS on the M/G/1 example against computation time, for various choices of N (number of importance samples) and M/N (ratio of target effective sampling size to N).

7.1. Model

We consider the time series model

$$x_{i+1} = x_i + \alpha(x_i, \theta)\Delta t + \sqrt{10\Delta t}\epsilon_i \quad (10)$$

$$\alpha(x_i, \theta) = \begin{pmatrix} \theta_1(x_{i,2} - x_{i,1}) \\ \theta_2 x_{i,1} - x_{i,2} - x_{i,1}x_{i,3} \\ x_{i,1}x_{i,2} - \theta_3 x_{i,3} \end{pmatrix}, \quad (11)$$

for $0 \leq i \leq m$. Here x_i is a vector $(x_{i,1}, x_{i,2}, x_{i,3})$ and $\epsilon_i \sim \mathcal{N}(0, I)$ is also a vector of length 3. This is a stochastic differential equation (SDE) version of the Lorenz 63 dynamical system (Lorenz, 1963) from Vrettas et al. (2015), after applying Euler-Maruyama discretisation.

We take $m = 100$ and assume independent observations $y_i \sim \mathcal{N}(x_i, \sigma^2 I)$ at $i = 20, 40, 60, 80, 100$. We fix $x_0 = (-30, 0, 30)$ and $\Delta t = 0.02$. The unknown parameters are $\theta = (\theta_1, \theta_2, \theta_3, \sigma)$. We simulate synthetic data from this discretised model for $\theta = (10, 28, 8/3, 2)$ – see Figure 4.

7.2. DIS implementation

Tempered target Our unnormalised tempered target is

$$\tilde{p}_\epsilon(\xi) = \pi(\theta)p(x|\theta)p(y|x, \theta)^{1-\epsilon}. \quad (12)$$

We initialise ϵ at 1. So the initial target p_1 is the prior and time series model unconditioned by y . As ϵ is reduced, more agreement with y is enforced.

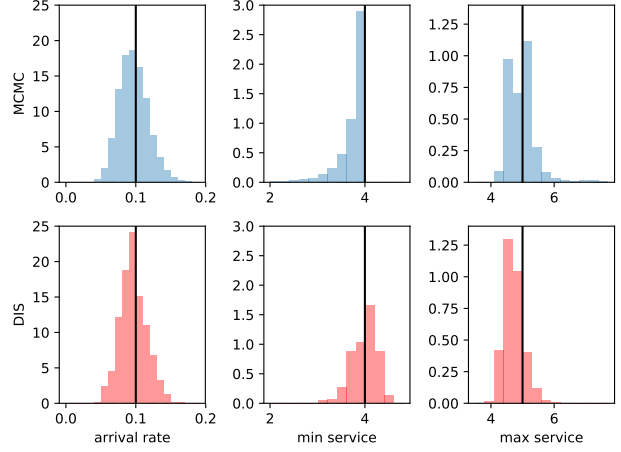


Figure 3. Marginal posterior histograms for M/G/1 example. Top: MCMC output. Bottom: DIS output after 180 minutes with $\epsilon = 0.283$.

Approximate family Following Ryder et al. (2018), we use an autoregressive approximate family

$$q(\xi; \phi) = q(\theta; \phi_\theta) \prod_{i=0}^{m-1} q(x_{i+1}|x_i, \theta; \phi_x).$$

We define $q(x_{i+1}|x_i, \theta; \phi_x)$ generatively as

$$x_{i+1} = x_i + [\alpha(x_i, \theta) + \beta]\Delta t + \sqrt{\gamma\Delta t}\epsilon_i. \quad (13)$$

This modifies (10) by adding to α an extra term β and replacing 10 with γ . We take β and γ to be outputs of a neural network with inputs (i, x_i, θ) and weights and biases ϕ_x . See Appendix D for more details.

In the limit $\Delta t \rightarrow 0$, interpreted in an appropriate fashion, (13) with $\gamma = 10$, and the correct choice of β , gives the conditional distribution $p(x|\theta, y)$ (see e.g. Opper, 2019). However, for $\Delta t > 0$ it is useful to allow γ to vary (Durham & Gallant, 2002). Intuitively the idea is that the random variation in $x_{i+1} - x_i$ may need to be smaller when $i + 1$ is close to an observation time, to ensure that the simulation is close to the observed value.

Tuning choices We use a real NVP architecture for $q(\theta; \phi_\theta)$, made up of 8 coupling layers, alternated with random permutation layers. Each coupling layer uses a neural network with 3 hidden layers of 30 units each and ELU activation. We can thus initialise $q(\theta; \phi_\theta)$ close to the prior $\pi(\theta)$ via the procedure described in Appendix B.

The network for β and γ has three hidden layers of 80 units each and ELU activation. We initialise the neural network to give x dynamics approximating those of the initial target p_1

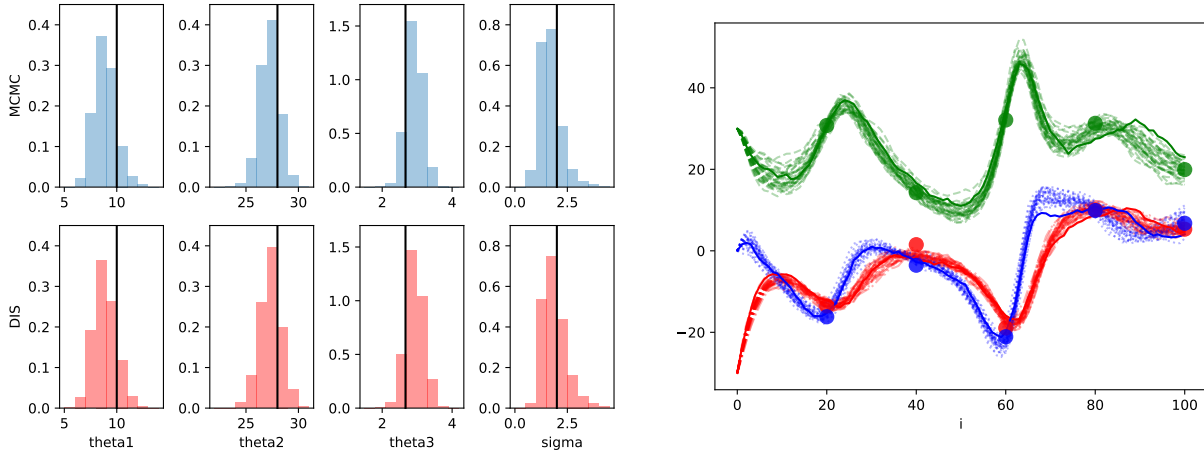


Figure 4. Output for Lorenz example with σ unknown. Left: marginal posterior histograms for parameters θ from particle MCMC and DIS output. Vertical lines show the true values. Right: paths x (red dot-dash $x_{i,1}$, blue dotted $x_{i,2}$, green dashed $x_{i,3}$) and observations (circles). Solid lines show the true paths. DIS plots are based on subsamples (1000 for θ , 30 for x) selected by resampling (see Section 3.3) from the final importance sampling output with $\epsilon = 0$, targeting the posterior distribution.

(the SDE without conditioning on y). See Appendix D for details. In this example, we used L_1 regularisation on neural network weights as we found this improved performance.

In the DIS algorithm we take $N = 50000$, $M = 2500$, following the general tuning suggestions in Section 6. See Appendix D for more details of tuning choices, and methods to avoid numerical instability.

Gradients The parameters for our approximating family are $\phi = (\phi_\theta, \phi_x)$. We calculate $\nabla_\phi \log q(\theta, x; \phi)$ by backpropagation. Simulating from q involves looping through (13) m times, each time using the neural network for β and γ . Backpropagation requires unrolling this. See Li et al. (2020) for recent progress on more efficient gradient calculation for SDE models.

7.3. Results

First we consider an example which is easy by other methods to verify that DIS gives correct results. Here we perform inference for θ under independent $\text{Exp}(0.1)$ priors on each θ_i and σ . Figure 4 shows the results using DIS, which takes 49 minutes and using particle MCMC (Andrieu et al., 2010), as detailed in Appendix F. The two methods produce very similar output, although MCMC is much faster, taking 4 minutes.

Secondly we investigate an example which is difficult for particle MCMC. Here we fix the observation scale to $\sigma = 0.2$, well below the true value of 2, and perform inference for $\theta_1, \theta_2, \theta_3$. Now DIS takes 443 minutes to target the posterior, Particle MCMC was infeasible with our available memory, but we estimate it would take at least 80,000 minutes. See

Appendices E and F for details.

These results illustrate that DIS can be implemented in a setting with high $\dim(x)$, and it outperforms MCMC methods for some problems. Also, unlike recent work in variational inference for SDEs (Ryder et al., 2018; Opper, 2019; Li et al., 2020), DIS directly targets the posterior distribution, not a variational approximation.

8. Conclusion

We’ve presented *distilled importance sampling*, and shown its application as an approximate Bayesian inference method for a likelihood-free example, and also as an exact method for a challenging time series model.

Limitations Variational inference scales well to large datasets, as it requires unbiased log-likelihood estimates, which can be calculated from small subsamples of data. DIS does not share this property, as the cost of each importance weight in DIS typically scales linearly with the size of the data e.g. by making a likelihood evaluation.

Also, we’ve focused on examples where evaluating \tilde{p}_ϵ is quick, and used many evaluations by taking N large. For more expensive models, this would be infeasible.

Finally, an occasional failure mode of our algorithm is that the distilled density can become too poor to produce low variance gradient estimates, and then cannot recover.

We hope these limitations can be addressed in future using ideas from the related work reviewed in Section 1. For instance reusing samples from earlier iterations may help

with the last two problems described.

Extensions There are interesting opportunities to extend DIS. It's not required that \tilde{p}_ϵ is differentiable, so discrete parameter inference is plausible. Also, we can use *random-weight importance sampling* (Fearnhead et al., 2010) in DIS, and replace \tilde{p}_ϵ with an unbiased estimate.

Acknowledgements Thanks to Alex Shestopaloff for providing MCMC code for the M/G/1 model and to Andrew Golightly and Chris Williams for helpful suggestions.

References

- Agapiou, S., Papaspiliopoulos, O., Sanz-Alonso, D., and Stuart, A. M. Importance sampling: Intrinsic dimension and computational cost. *Statistical Science*, 32(3):405–431, 2017.
- Andrieu, C., Doucet, A., and Holenstein, R. Particle Markov chain Monte Carlo methods. *Journal of the Royal Statistical Society: Series B*, 72(3):269–342, 2010.
- Baydin, A. G., Shao, L., Bhimji, W., Heinrich, L., Naderiparizi, S., Munk, A., Liu, J., Gram-Hansen, B., Louppe, G., Meadows, L., Torr, P., Lee, V., Cranmer, K., Prabhat, and Wood, F. Efficient probabilistic inference in the quest for physics beyond the standard model. In *Advances in Neural Information Processing Systems*, 2019.
- Cappé, O., Guillin, A., Marin, J.-M., and Robert, C. P. Population Monte Carlo. *Journal of Computational and Graphical Statistics*, 13(4):907–929, 2004.
- Chatterjee, S. and Diaconis, P. The sample size required in importance sampling. *The Annals of Applied Probability*, 28(2):1099–1135, 2018.
- Cornuet, J.-M., Marin, J.-M., Mira, A., and Robert, C. P. Adaptive multiple importance sampling. *Scandinavian Journal of Statistics*, 39(4):798–812, 2012.
- Cotter, S. L., Kevrekidis, I. G., and Russell, P. Transport map accelerated adaptive importance sampling, and application to inverse problems arising from multiscale stochastic reaction networks. *arXiv preprint arXiv:1901.11269*, 2019.
- Del Moral, P., Doucet, A., and Jasra, A. Sequential Monte Carlo samplers. *Journal of the Royal Statistical Society: Series B*, 68(3):411–436, 2006.
- Del Moral, P., Doucet, A., and Jasra, A. An adaptive sequential Monte Carlo method for approximate Bayesian computation. *Statistics and Computing*, 22(5):1009–1020, 2012.
- Dieng, A. B., Tran, D., Ranganath, R., Paisley, J., and Blei, D. Variational inference via χ upper bound minimization. In *Advances in Neural Information Processing Systems*, 2017.
- Dinh, L., Sohl-Dickstein, J., and Bengio, S. Density estimation using real NVP. *arXiv preprint arXiv:1605.08803*, 2016.
- Doucet, A., Pitt, M. K., Deligiannidis, G., and Kohn, R. Efficient implementation of Markov chain Monte Carlo when using an unbiased likelihood estimator. *Biometrika*, 102(2):295–313, 2015.
- Duan, L. L. Transport Monte Carlo. *arXiv preprint arXiv:1907.10448*, 2019.
- Durham, G. B. and Gallant, A. R. Numerical techniques for maximum likelihood estimation of continuous-time diffusion processes. *Journal of Business & Economic Statistics*, 20(3):297–338, 2002.
- Fearnhead, P., Papaspiliopoulos, O., Roberts, G. O., and Stuart, A. Random-weight particle filtering of continuous time processes. *Journal of the Royal Statistical Society: Series B*, 72(4):497–512, 2010.
- Graham, M. M. and Storkey, A. J. Asymptotically exact inference in differentiable generative models. *Electronic Journal of Statistics*, 11(2):5105–5164, 2017.
- Grazian, C. and Fan, Y. A review of approximate Bayesian computation methods via density estimation: Inference for simulator-models. *Wiley Interdisciplinary Reviews: Computational Statistics*, 2019.
- Green, P. J., Łatuszyński, K., Pereyra, M., and Robert, C. P. Bayesian computation: a summary of the current state, and samples backwards and forwards. *Statistics and Computing*, 25(4):835–862, 2015.
- Ionides, E. L. Truncated importance sampling. *Journal of Computational and Graphical Statistics*, 17(2):295–311, 2008.
- King, A. A., Nguyen, D., and Ionides, E. L. Statistical inference for partially observed Markov processes via the R package pomp. *Journal of Statistical Software*, 69(12), 2016.
- Larrañaga, P. and Lozano, J. A. *Estimation of distribution algorithms: A new tool for evolutionary computation*. Springer, 2002.
- Le, T. A., Baydin, A. G., and Wood, F. Inference compilation and universal probabilistic programming. In *Artificial Intelligence and Statistics*, 2017.

- Li, X., Wong, T.-K. L., Chen, R. T. Q., and Duvenaud, D. Scalable gradients for stochastic differential equations. In *Artificial Intelligence and Statistics*, 2020.
- Li, Y., Turner, R. E., and Liu, Q. Approximate inference with amortised MCMC. *arXiv preprint arXiv:1702.08343*, 2017.
- Lindley, D. V. The theory of queues with a single server. *Mathematical Proceedings of the Cambridge Philosophical Society*, 48(2):277–289, 1952.
- Liu, J. S. Metropolisized independent sampling with comparisons to rejection sampling and importance sampling. *Statistics and Computing*, 6(2):113–119, 1996.
- Lorenz, E. N. Deterministic nonperiodic flow. *Journal of the atmospheric sciences*, 20(2):130–141, 1963.
- Marin, J.-M., Pudlo, P., Robert, C. P., and Ryder, R. J. Approximate Bayesian computational methods. *Statistics and Computing*, 22(6):1167–1180, 2012.
- Mohamed, S., Rosca, M., Figurnov, M., and Mnih, A. Monte Carlo gradient estimation in machine learning. *arXiv preprint arXiv:1906.10652*, 2019.
- Müller, T., McWilliams, B., Rousselle, F., Gross, M., and Novák, J. Neural importance sampling. *arXiv preprint arXiv:1808.03856*, 2018.
- Opper, M. Variational inference for stochastic differential equations. *Annalen der Physik*, 531(3):1800233, 2019.
- Papamakarios, G. and Murray, I. Fast ε -free inference of simulation models with Bayesian conditional density estimation. In *Advances in Neural Information Processing Systems*, 2016.
- Papamakarios, G., Nalisnick, E., Rezende, D. J., Mohamed, S., and Lakshminarayanan, B. Normalizing flows for probabilistic modeling and inference. *arXiv preprint arXiv:1912.02762*, 2019a.
- Papamakarios, G., Sterratt, D., and Murray, I. Sequential neural likelihood: Fast likelihood-free inference with autoregressive flows. In *Artificial Intelligence and Statistics*, 2019b.
- Parno, M. D. and Marzouk, Y. M. Transport map accelerated Markov chain Monte Carlo. *SIAM/ASA Journal on Uncertainty Quantification*, 6(2):645–682, 2018.
- Pascanu, R., Mikolov, T., and Bengio, Y. On the difficulty of training recurrent neural networks. In *International Conference on Machine Learning*, 2013.
- Robert, C. P. and Casella, G. *Monte Carlo statistical methods*. Springer, 2013.
- Rubinstein, R. The cross-entropy method for combinatorial and continuous optimization. *Methodology and computing in applied probability*, 1(2):127–190, 1999.
- Rubinstein, R. Y. and Kroese, D. P. *Simulation and the Monte Carlo method*. John Wiley & Sons, 2016.
- Ruiz, F. and Titsias, M. A contrastive divergence for combining variational inference and MCMC. In *International Conference on Machine Learning*, 2019.
- Ryder, T., Golightly, A., McGough, A. S., and Prangle, D. Black-box variational inference for stochastic differential equations. In *International Conference on Machine Learning*, 2018.
- Sherlock, C., Thiery, A. H., Roberts, G. O., and Rosenthal, J. S. On the efficiency of pseudo-marginal random walk Metropolis algorithms. *The Annals of Statistics*, 43(1): 238–275, 2015.
- Shestopaloff, A. Y. and Neal, R. M. On Bayesian inference for the M/G/1 queue with efficient MCMC sampling. *arXiv preprint arXiv:1401.5548*, 2014.
- Smith, A. F. M. and Gelfand, A. E. Bayesian statistics without tears: a sampling–resampling perspective. *The American Statistician*, 46(2):84–88, 1992.
- Turner, R. E., Berkes, P., Sahani, M., and MacKay, D. J. C. Counterexamples to variational free energy compactness folk theorems. Technical report, University College London, 2008.
- Vats, D., Flegal, J. M., and Jones, G. L. Multivariate output analysis for Markov chain Monte Carlo. *Biometrika*, 106(2):321–337, 2019.
- Vrettas, M. D., Opper, M., and Cornford, D. Variational mean-field algorithm for efficient inference in large systems of stochastic differential equations. *Physical Review E*, 91, 2015.
- Whitaker, G. A., Golightly, A., Boys, R. J., and Sherlock, C. Improved bridge constructs for stochastic differential equations. *Statistics and Computing*, 27(4):885–900, 2017.
- Wilkinson, R. D. Approximate Bayesian computation (ABC) gives exact results under the assumption of model error. *Statistical applications in genetics and molecular biology*, 12(2):129–141, 2013.
- Yao, Y., Vehtari, A., Simpson, D., and Gelman, A. Yes, but did it work?: Evaluating variational inference. In *International Conference on Machine Learning*, pp. 5577–5586, 2018.

A. Truncating importance weights

Importance sampling estimates can have large or infinite variance if λ is a poor approximation to p . The practical manifestation of this is a small number of importance weights being very large relative to the others. To reduce the variance, Ionides (2008) introduced *truncated importance sampling*. This replaces each importance weight w_i with $\tilde{w}_i = \min(w_i, \omega)$ given some threshold ω . The truncated weights are then used in estimates (3) or (4). Truncating in this way typically reduces variance, at the price of increasing bias.

Gradient clipping (Pascanu et al., 2013) is common practice in stochastic gradient optimisation of an objective $\mathcal{J}(\phi)$ to prevent occasional large gradient estimates from destabilising optimisation. Truncating importance weights in Algorithm 1 has a similar effect of reducing the variability of gradient estimates. A potential drawback of either method is that gradients lose the property of unbiasedness, which is theoretically required for convergence to an optimum of the objective. Pascanu et al. (2013) give heuristic arguments for good optimiser performance when using truncated gradients, and we make the following similar case for using clipped weights. Firstly, even after truncation, the gradient is likely to point in a direction increasing the objective. In our approach, it should still increase the q density at $\xi^{(i)}$ values with large w_i weights, which is desirable. Secondly, we expect there is a region near the optimum for ϕ where truncation is extremely rare, and therefore gradient estimates have very low bias once this region is reached. Finally, we also observe good empirical behaviour in our examples, showing that optimisation with truncated weights can find very good importance sampling proposals.

We could use gradient clipping directly in Algorithm 1. However we prefer truncating importance weights as there is an automated way to choose the threshold ω , as follows. We select ω to reduce the maximum normalised importance weight, $\max_i \frac{\tilde{w}_i}{\sum_{i=1}^N \tilde{w}_i}$, to a prespecified value: throughout we use 0.1. The required ω can easily be calculated e.g. by bisection. (Occasionally no such ω exists i.e. if most w_i s are zero. In this case we set ω to the smallest positive w_i .)

B. Approximate density initialisation

As discussed in Section 4.1, we wish to initialise $q(\xi; \phi)$ close to its initial target distribution p_{ϵ_0} . This avoids importance sampling initially producing high variance gradient estimates.

An approach we use in our examples is to select real NVP parameters so that all its coupling layers are approximately the identity transformation. Then the resulting distribution approximates its base distribution $\mathcal{N}(0, I)$. We can often design our initial target to equal this, or to be sufficiently

similar that only a few iterations of pretraining are needed.

To achieve this we initialise all the neural network weights and biases used in real NVP to be approximately zero. In more detail, we set biases to zero and sample weights from $\mathcal{N}(0, 0.001^2)$ distributions truncated to two standard deviations from the mean. We also ensure that we use activation functions which map zero to zero. Then the neural network outputs μ and σ are also approximately zero. Thus each coupling layer has shift vector $\mu \approx 0$ and scale vector $\exp(\sigma) \approx 1$.

C. M/G/1 model

This section describes the M/G/1 queueing model, in particular how to simulate from it.

Recall that the parameters are $\theta_1, \theta_2, \theta_3$, with independent prior distributions $\theta_1 \sim U(0, 1/3)$, $\theta_2 \sim U(0, 10)$, $\theta_3 - \theta_2 \sim U(0, 10)$. We introduce a reparameterised version of our parameters: $\vartheta_1, \vartheta_2, \vartheta_3$ with independent $\mathcal{N}(0, 1)$ priors. Then we can take $\theta_1 = \Phi^{-1}(\vartheta_1)/3$, $\theta_2 = 10\Phi^{-1}(\vartheta_2)$ and $\theta_3 = \theta_2 + 10\Phi^{-1}(\vartheta_3)$, where Φ is the $\mathcal{N}(0, 1)$ cumulative distribution function.

The model involves independent latent variables $x_i \sim \mathcal{N}(0, 1)$ for $1 \leq i \leq 2m$, where m is the number of observations. These generate

$$a_i = -\frac{1}{\theta_3} \log \Phi^{-1}(x_i), \quad (\text{inter-arrival times})$$

$$s_i = \theta_2 + (\theta_3 - \theta_2)\Phi^{-1}(x_{i+m}). \quad (\text{service times})$$

Inter-departure times can be calculated through the following recursion (Lindley, 1952)

$$d_i = s_i + \max(A_i - D_{i-1}), \quad (\text{inter-departure times})$$

where $A_i = \sum_{j=1}^i a_j$ (arrival times) and $D_i = \sum_{j=1}^i d_j$ (departure times).

D. Lorenz example tuning details

Here we describe further details of our implementation of DIS for the Lorenz example.

Numerical stability The Lorenz model (10) can produce large x_i values which cause numerical difficulties in our implementation. To avoid this our code gives zero importance weight to any simulation where $\max_{i,j} |x_{i,j}| > 1000$. Effectively this is a weak extra prior constraint. Our final posteriors in Figures 4 and 5 shows no x_i values near this bound, verifying that this constraint has a negligible effect on the final results.

Neural network input The inputs to the neural network for β and γ , used in (13), are:

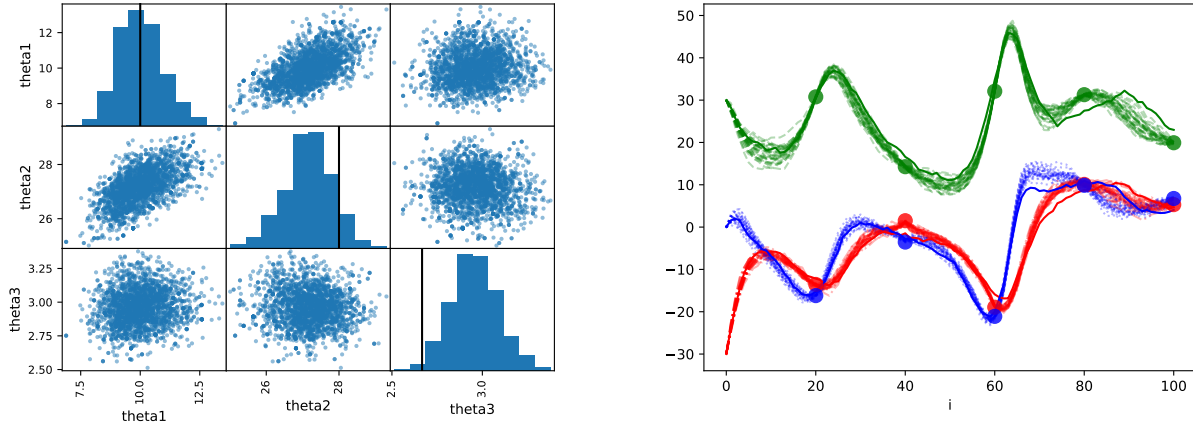


Figure 5. Output for Lorenz example with $\sigma = 0.2$. Left: Parameters θ . Diagonal plots show histograms of marginals, with vertical lines showing the true values. Off-diagonal plots show bivariate scatter-plots. Right: Paths x (red dot-dash $x_{i,1}$, blue dotted $x_{i,2}$, green dashed $x_{i,3}$) and observations (dots). Solid lines show the true paths. Both panels are subsamples (1000 left, 30 right) selected by resampling (see Section 3.3) from the final importance sampling output with $\epsilon = 0$, targeting the posterior distribution. Darker points/lines indicate more frequent resampling.

- Parameters θ
- Current time i
- Current state x_i

and also the following derived features:

- Current $\alpha(x_i, \theta)$, from (11)
- Time until next observation
- Next observation value

Neural network initialisation and output As discussed in Section 7, we aim to initialise the neural network for β and γ so that (13) produces x dynamics similar to those of the initial target. This requires $\beta \approx (0, 0, 0)$ and $\gamma \approx 10$. To achieve this we initialise as follows.

We initialise the biases to zero and the weights close to zero, as in Appendix B. Our final neural network layer has 4 outputs. Under our initialisation these will be close to zero. Three are used as β , providing the required initial values. The remaining output of the neural network, η , is used to produce the multiplier γ through

$$\gamma = \frac{10}{\log(2)} \text{softplus}(\eta).$$

We apply the softplus transform since γ must be positive. The constant factor ensures that $\eta = 0$ produces $\gamma = 10$, as required.

E. DIS results for fixed σ Lorenz example

Figure 5 shows the DIS results in the Lorenz example with σ fixed at 0.2. The results shown are after 1500 iterations, taking 652 minutes.

F. Particle MCMC analysis of Lorenz examples

As a comparison to DIS, we also investigate inference for the Lorenz example using particle Markov chain Monte Carlo (PMCMC) (Andrieu et al., 2010), a near-exact inference method. This runs a Metropolis-Hastings MCMC algorithm for the model parameters θ . For each proposed θ , the likelihood is estimated by running a particle filter for the x variables with N_{PF} particles. A particle filter involves forward simulating the unconditioned time series model to the next observation time and weighting the simulated paths based on the density of the observation given the endpoint. We implement PMCMC and particle filters using the `pomp` R package (King et al., 2016).

One PMCMC tuning choice is the proposal distribution for θ . We use a normal proposal, with variance equal to a posterior covariance matrix estimate from a pilot PMCMC run. Another choice is where to initialise the MCMC chain. For simplicity we use the true parameter values. In a real analysis initialisation is often more difficult.

A key remaining tuning choice is selecting N_{PF} so that the particle filter produces likelihood estimates which are accurate enough for the MCMC algorithm to be efficient. We follow the theoretically derived tuning advice of Sherlock et al. (2015) and Doucet et al. (2015): we choose N_{PF} so that the log-likelihood estimates at a representative parameter value (we use the true parameter values) have a standard deviation s of roughly 1.5.

In our first example σ , observation noise scale, is an un-

known parameter whose true value is 2. For $\sigma = 2$ it is relatively common for forward simulations to produce high observation densities. This is reflected in that we need only $N_{PF} = 50$ to attain $s \approx 1.5$, and so PMCMC was fast to run. We ran 80,000 PMCMC iterations, taking 4 minutes. This produces an effective sample size – calculated using the method of Vats et al., 2019 – of 2328, comparable to the target ESS of 2500 used by DIS.

However in our second example we fix $\sigma = 0.2$. At this level noise it is rare for forward simulations to produce high observation densities, particularly for the observations in Figure 4 which lie furthest from the true paths. Hence even $N_{PF} = 10^6$, near the largest choice we could use with our available memory, produced $s \approx 6$. We can estimate a lower bound on the time cost of PMCMC for this example without memory constraints by considering how long 10^6 particles would take. The computational cost of this particle filter implementation is $O(N_{PF})$ (King et al., 2016), and using 50 particles in PMCMC took 4 minutes. So MCMC using 10^6 particles would take approximately $4 \times 10^6 / 50 = 80,000$ minutes, which is orders of magnitude longer than DIS.

G. Algorithm complexity

The nominal computational complexity of our DIS algorithm is $O(TN)$, where T is the number of iterations of the main loop performed. Recall that N is the number of samples used in importance sampling. However the cost required to reach a given value of ϵ is more complicated. Figure 2 investigated its dependence on N and M (the target ESS value). It will also depend on many other tuning choices such as: the approximate family used for q ; initialisation and pretraining; number (B) and size (n) of training batches. Further investigation how to optimally tune these is an interesting topic for future work.

Storage costs will be dominated by: storage of ϕ and N w_i weights; backpropagation costs; and application-specific calculations needed for \tilde{p}_ϵ . Improvements which reduce the required IS sample size and number of neural network parameters will benefit both computational and storage complexity.